

# Two-component approach for thermodynamic properties in diluted magnetic semiconductors

Malcolm P. Kennett<sup>1</sup>, Mona Berciu<sup>2</sup> and R. N. Bhatt<sup>1,2</sup>

<sup>1</sup>*Department of Physics and* <sup>2</sup>*Department of Electrical Engineering, Princeton University, Princeton, NJ 08544*  
(October 29, 2018)

We examine the feasibility of a simple description of Mn ions in III-V diluted magnetic semiconductors (DMSs) in terms of two *species* (components), motivated by the expectation that the Mn-hole exchange couplings are widely distributed, especially for low Mn concentrations. We find, using distributions indicated by recent numerical mean field studies, that the thermodynamic properties (magnetization, susceptibility, and specific heat) cannot be fit by a single coupling as in a homogeneous model, but can be fit well by a two-component model with a temperature dependent number of “strongly” and “weakly” coupled spins. This suggests that a two-component description may be a minimal model for the interpretation of experimental measurements of thermodynamic quantities in III-V DMS systems.

PACS: 75.50.Pp, 75.10.Lp, 75.40.-s, 75.30.Hx

## I. INTRODUCTION

Diluted, magnetic semiconductors (DMSs) have been the focus of intense study recently due to their potential for use in novel devices making use of both magnetic and conventional semiconductor properties.<sup>1,2</sup> The discovery of a magnetic transition temperature,  $T_c$ , of 110 K in a sample of  $\text{Ga}_{1-x}\text{Mn}_x\text{As}$  for  $x = 0.053$  has further spurred efforts to understand the origin and physical effects that influence the magnetic properties of these materials.<sup>3</sup>

It is now reasonably well established that III-V systems such as  $\text{Ga}_{1-x}\text{Mn}_x\text{As}$  with  $x = 0.01 - 0.07$  are itinerant ferromagnets, in which the Mn ions play the dual roles of acceptor site and magnetic ion, and the itinerant carriers are holes, which have an antiferromagnetic interaction with the Mn spins.<sup>4-8</sup> The antiferromagnetic hole-Mn interaction leads to an effective ferromagnetic interaction between Mn spins, and gives rise to the ferromagnetic transition. One experimental fact that may be of importance is that in these systems the number of holes  $n_h$  is only a small fraction of the number of Mn dopants (or Mn spins),  $n_{\text{Mn}}$ , implying that the system has low carrier density, and is heavily compensated.

Theoretically, there have been several approaches to trying to calculate the thermodynamic and transport properties of these materials – one approach has been to look at the effect of spin waves<sup>9-11</sup> whilst another has been a mean field model including spin-orbit effects.<sup>4</sup> Both of these approaches leave out the disorder due to the random positions of the Mn ions in the sample. The effect of random positions has been considered in a numerical mean field theory<sup>12,13</sup> for the low density phase of  $\text{Ga}_{1-x}\text{Mn}_x\text{As}$ , as well as in Monte Carlo simulations of the insulating phase of II-VI DMS, represented by a Heisenberg model for the Mn and carrier spins.<sup>14,15</sup> Both of these investigations show that the positional disorder gives rise to a distribution of exchange couplings between Mn ions and holes. Monte Carlo results have also been obtained for a model in which the hole-Mn coupling is assumed constant and leads to an effective Mn-Mn in-

teraction where positional disorder is included.<sup>16</sup> A recent Monte Carlo study of  $\text{Ga}_{1-x}\text{Mn}_x\text{As}$  using a kinetic-exchange model,<sup>17</sup> has appeared whilst this work was being written up.

In this paper, we construct the simplest mean field model that attempts to capture the effects of disorder in the effective local fields at different Mn sites. This disorder arises as a result of the different local potential for the carrier at different Mn sites. At one extreme we consider a simple model of compensation by antisite defects. In this model, each As antisite defect is viewed as capturing the holes of two neighboring Mn dopants, and providing an onsite potential that is significantly different from Mn sites that are far from such As antisites. This naturally leads to description of the Mn spins in terms of two distinct species. This is clearly a caricature, since for positionally random doping and As antisite defects, there will be a *continuous distribution* of onsite potentials rather than a bimodal one. However, as we show in the bulk of our paper, if the distribution is rather wide (as is found in the mean-field study of Mn impurity bands<sup>12,13</sup>), such a bimodal distribution provides a reasonable description of the thermodynamics, provided we allow the relative weights of the two species to be temperature dependent according to a simple rule, which occurs naturally in the analysis.

We concentrate only on the carrier-spin exchange part of the Hamiltonian, since a numerical mean-field treatment<sup>13</sup> shows that this term captures most of the condensation energy for the magnetic phase, and the carrier kinetic energy changes only weakly with the onset of ferromagnetism. As stated earlier, in the regime of interest, the concentration of holes,  $n_h$ , is considerably less than the concentration  $n_{\text{Mn}}$  of Mn ions. The fluctuations in the local carrier charge density (due to fluctuations in the occupation number of the impurity states around Mn sites with different surroundings) are then represented by a fluctuation of the effective exchange coupling between the Mn moment and the spin of the carrier.

Our results can be summarized simply as follows : we

find that representing the hole-Mn antiferromagnetic exchange coupling by a *single* parameter is insufficient to capture the thermodynamic behaviour, such as the temperature dependence of the magnetization, susceptibility and specific heat in the ferromagnetic phase, when disorder is large. However, by using a model where there are two species of Mn ions, with different hole-Mn exchange couplings, we are able to fit the magnetization and other thermodynamic parameters that we calculate from a distribution of couplings in a much more satisfactory manner. Furthermore, as argued below, such a two-component model captures the inadequacies of the homogeneous model in a manner that is qualitatively correct for temperatures not too close to  $T_c$ . *We emphasize that the label “component” used throughout this paper, is synonymous with “species” or “type”, and has no relation to the number of components of the spin itself, which in this work refers to a vector in three dimensions.*

The idea of using a two-component model is similar in spirit to models developed to understand the magnetic behaviour of doped non-magnetic semiconductors such as phosphorus doped silicon, motivated by the observation that exchange couplings in such systems should be distributed over many orders of magnitude.<sup>18,19</sup> In Mn doped DMS systems, disorder appears to lead to a similar situation of widely distributed couplings.<sup>13</sup> Whilst not explicitly included in Refs. 12,13 the large compensation, apparently from As antisite defects, would enhance disorder, and hence broaden the distribution of effective couplings. Therefore a two component approach appears to be a natural approximation that is qualitatively correct, and may be quantitatively adequate for many purposes.

## II. MEAN FIELD MODEL

### A. Hamiltonian

The DMS system we study consists of magnetic ions (Mn) coupled to charge carriers. In the case of II-VI semiconductors (e.g. ZnSe), the carrier is provided by a second dopant (such as P); however, in III-V semiconductors (e.g. GaAs), Mn, being a divalent atom substituting on a trivalent (Ga) site, provides a hole in addition to the spin. In this paper, we use the example of  $\text{Ga}_{1-x}\text{Mn}_x\text{As}$  for concreteness.

For Mn concentrations of interest (a fraction of a percent to a few percent), and hole concentrations of about 10%-20% per Mn impurity, the system is near a metal-insulator transition (MIT).<sup>6,20</sup> This implies that the hole wavefunctions are filamentary, with a multifractal structure on length scales that determine the magnetic behaviour of the system, which is quite distinct from the homogeneous structure for plane wave (or Bloch wave) states characteristic of periodic systems. Thus, each hole interacts with many Mn spins, depending on the amplitude of its wavefunction at various Mn sites, as well as the

envelope function characterizing the hole. Since each hole interacts with a large number of spins the net exchange fields felt by different holes are similar (i.e., the fluctuations are not that large). However, the hole concentration is considerably (a factor of 5-10) smaller than the Mn concentration; therefore, each Mn spin experiences a rather different exchange field due to the few holes that have significant amplitude at that site (or nearby sites, via the tail of the envelope function). Hence the fluctuations in the local exchange field at different Mn sites *cannot* be ignored, since the fields are being produced predominantly by just a few holes. This asymmetry has been documented in a numerical study<sup>13</sup> and forms the basis of our simple phenomenological scheme. These fluctuations are of paramount importance in the insulating phase and at the MIT. If experience with conventional doped semiconductors is any guide, they are likely to persist well into the metallic phase<sup>12,19</sup> and cannot reasonably be ignored in any theory of DMS ferromagnetism up to dopant densities well above (a factor of 3-5) the dopant density for the MIT. The above discussion raises questions about the applicability of the results of studies which are based on homogeneous mean-field models, as well as those based on perturbative treatments of the Mn spin system (such as RKKY exchange), given the large ratio of spin to carrier density.

The diluteness of the carrier system leads us to neglect hole-hole interactions. Direct Mn-Mn interactions are also ignored because they are extremely short range due to the atomic nature of the Mn 3d-orbitals responsible for the Mn spin. Furthermore, the numerical mean field treatment<sup>13</sup> shows that the energy gain due to the onset of ferromagnetic ordering coming from the exchange term in the Hamiltonian is much larger than the change in carrier kinetic energy. Ignoring the kinetic energy is not expected to lead to any major qualitative differences. In fact, in our results it does not lead to even *quantitative* differences in the magnetization for temperatures below about  $0.6 T_c$  (as shown in Section III), while there are quantitative differences nearer the ordering temperature, as the exchange energy and kinetic energy variations with  $T$  become comparable in magnitude. Consequently, in keeping with the philosophy of finding a minimal model description, we consider only the exchange term of the Hamiltonian in this paper. This Hamiltonian takes a form similar to that studied by König *et al.*<sup>9</sup> with no kinetic term:

$$\mathcal{H} = \int d^3\mathbf{r} \sum_{i,\alpha} J_{i\alpha}(\mathbf{r}) \mathbf{s}_\alpha \cdot \mathbf{S}_i(\mathbf{r}) - \int d^3\mathbf{r} \left\{ g\mu_B \mathbf{B} \cdot \sum_i \mathbf{S}_i(\mathbf{r}) + g^* \mu_B \mathbf{B} \cdot \sum_\alpha \mathbf{s}_\alpha(\mathbf{r}) \right\}, \quad (1)$$

where  $\alpha$  labels the holes,  $i$  labels the Mn spins,  $\mathbf{s}_\alpha$  is the spin for the  $\alpha^{\text{th}}$  hole and  $\mathbf{S}_i(\mathbf{r})$  is the Mn spin centered on site  $i$ . The g-factors of the hole and Mn spins are labelled by  $g^*$  and  $g$  respectively,  $\mu_B$  is the Bohr magneton and

$\mathbf{B}$  is an external magnetic field, which we shall assume to be zero unless otherwise stated. The overlap integral for the  $\alpha^{th}$  hole with the spin centered on site  $i$  is  $J_{i\alpha}$ . We assume that the d-electrons that give rise to the Mn spins are localized in comparison to the holes and treat the Mn spins as having delta function spatial dependence, i.e.  $\mathbf{S}_i(\mathbf{r}) = \mathbf{S}_i \delta^{(3)}(\mathbf{r} - \mathbf{R}_i)$ , which, after integrating out the delta functions, leads to the Hamiltonian

$$\mathcal{H} = \sum_i \sum_{\alpha} J_{i\alpha}(\mathbf{R}_i) \mathbf{s}_{\alpha} \cdot \mathbf{S}_i, \quad (2)$$

where  $J_{i\alpha}(\mathbf{R}_i) = J_0 |\phi_{\alpha}(\mathbf{R}_i)|^2$ , with  $\phi_{\alpha}(\mathbf{r})$  the wavefunction of the  $\alpha^{th}$  hole and  $J_0$  the microscopic exchange constant. We can write  $\sum_{\alpha} J_{i\alpha}(\mathbf{R}_i) \mathbf{s}_{\alpha} = \mathbf{h}(\mathbf{R}_i)$ , and treat the effect of the magnetization of the hole spins as creating an effective field at each Mn site, so our Hamiltonian is

$$\mathcal{H} = \sum_i \mathbf{h}(\mathbf{R}_i) \cdot \mathbf{S}_i. \quad (3)$$

In a recent mean-field study<sup>13</sup> of a tight-binding model of the impurity band arising from holes on Mn sites coupled to Mn spins, the randomness of the Mn sites is explicitly taken into account. That work involves a numerical implementation of the self-consistent mean field equations, in which the effective fields are self-consistently calculated at *each* Mn site for each temperature,  $T$ . (The mean-field in such treatments refers only to temporal averaging over the local environment, and not positional averaging). A ferromagnetic phase is found below a critical temperature, with a *distribution* of effective fields,  $P(h)$ , which is temperature dependent. The numerical mean field model explicitly includes the itinerant nature of the holes. We use the distribution of effective fields from the self-consistent mean-field calculations. Hence, even though the models constructed here are in the form of pure exchange, the wavefunctions used to calculate effective couplings are those of itinerant electrons. Consequently, that physics is implicit in these models. In a mean field description of carrier moments, the field is simply a product of the mean moment (which we take to be along the  $z$  direction, of magnitude  $s^z$ ) and an effective exchange interaction  $J$  which varies from site to site. Thus, we can obtain from the numerical study, an effective distribution of exchange couplings  $P(J)$ , and our Hamiltonian becomes an integral over the distribution  $P(J)$ :

$$\mathcal{H}_{\text{distribution}} = \int_0^{J_{\text{max}}} dJ P(J) J S_j^z s^z. \quad (4)$$

Details of the derivation are given in Appendix A.

In a fully self-consistent scheme (such as Ref. 12) the distribution  $P(J)$  depends on the temperature  $T$  due to the temperature dependence of the hole amplitude distribution. However, as we show below, the distribution

$P_0(J)$  calculated at  $T = 0$  works very well for temperatures up to  $T = 0.6 T_c$ . Hence, in keeping with our search for a *simple* model, we will use  $P_0(J)$ , and consider the  $T$ -dependence of  $P(J)$  only where necessary.

### 1. Spin and carrier magnetization

We find a self-consistent solution for the average Mn spin of

$$\langle S_j^z \rangle = -S B_S(\beta \alpha_J), \quad (5)$$

where  $S = 5/2$  is the spin of each Mn ion,

$$B_S(x) = \frac{2S+1}{2S} \coth\left(\frac{2S+1}{2}x\right) - \frac{1}{2S} \coth\left(\frac{x}{2}\right), \quad (6)$$

is the Brillouin function for spins with magnitude  $S$  and

$$\alpha_J = J \langle s^z \rangle. \quad (7)$$

We also need to take into account the fact that the holes experience an effective field from the Mn spins, which leads to the following self-consistency condition

$$\langle s^z \rangle = -j B_j(\beta \alpha^*), \quad (8)$$

where

$$\alpha^* = \frac{1}{p} \int_0^{J_{\text{max}}} dJ P(J) J \langle S_j^z \rangle, \quad (9)$$

$p$  is the ratio  $n_h/n_{\text{Mn}}$  and  $j$  is the effective hole spin ( $j = 3/2$  in real systems). To compare our results with the numerical study,<sup>12,13</sup> we use the Brillouin function with  $j = 1/2$  for the hole spin and replace  $J_0$  by  $3J_0$  so that in effect the hole spins take values of  $\pm 3/2$ . We emphasize however, that we have found that treating the spin as a classical object (i.e. using a Langevin function) or using Brillouin functions with  $j = 1/2$  or  $j = 3/2$  does not affect the basic picture we have here, or the characteristic *shape* of the curves, other than in raising or lowering  $T_c$ . The value of  $T_c$  is given by

$$T_c = \sqrt{\frac{35}{48} p \overline{J^2}}, \quad (10)$$

where  $\overline{\dots}$  denotes an average with respect to  $P(J)$  and  $\langle \dots \rangle$  denotes a thermodynamic average. Note that whilst  $p$  enters Equation (10) explicitly, there is also an implicit dependence, in that  $p$  affects the distribution of hole-Mn exchange couplings  $P(J)$  and hence  $\overline{J^2}$ .

### 2. Susceptibility and Specific Heat

We next calculate the magnetic susceptibility and specific heat at zero field. The susceptibility per unit volume is

$$\chi = \chi^* + \int_0^{J_{\max}} dJ \chi_J, \quad (11)$$

where  $\chi^*$  is the contribution to the susceptibility due to the holes and  $\chi_J$  is the contribution to the susceptibility from Mn spins coupled to holes with exchange  $J$ . The individual expressions for the susceptibilities are

$$\chi^* = \frac{(g^* \mu_B)^2 n_h \beta G^* \left(1 - \frac{g}{g^*} \frac{\beta}{p} \int_0^{J_{\max}} dJ P(J) J G_J\right)}{1 - \frac{1}{p} \beta^2 G^* \int_0^{J_{\max}} dJ P(J) J^2 G_J}, \quad (12)$$

$$\chi_J = g \mu_B P(J) n_{\text{Mn}} \beta G_J \left(g \mu_B - \frac{1}{n_h} \frac{J}{g^* \mu_B} \chi^*\right), \quad (13)$$

where

$$G^* = j \frac{d}{dx} [B_j(x)]_{x=\beta \alpha^*}, \quad (14)$$

$$G_J = S \frac{d}{dx} [B_S(x)]_{x=\beta \alpha_J}. \quad (15)$$

We use the expressions for the susceptibility given in equations (12) and (13) with  $g = 2$ , and assume  $g^* = 2$  for our numerical calculations in section III.<sup>21</sup>

To obtain the specific heat we have to be careful since we calculate with a Hamiltonian that has temperature dependent coefficients and the concentrations of strongly and weakly coupled spins may also depend on temperature. We use the mean field free energy to obtain the specific heat through the relation

$$C_V = \frac{dU}{dT}, \quad (16)$$

where we note that the energy per Mn spin is

$$\frac{U}{N_{\text{Mn}}} = \int_0^{J_{\max}} dJ P(J) J \langle S_J^z \rangle \langle s^z \rangle, \quad (17)$$

in our mean field theory, where  $N_{\text{Mn}}$  is the total number of Mn spins.

## B. Single and two component models

For a system without disorder, the exchange between carriers and spins can be characterized by a single coupling, as has been done, *e.g.*, in Ref. 9. To demonstrate how these models are inadequate for the system under consideration, we consider two simplified models to substitute for the hierarchy of couplings implied by the distribution  $P_0(J)$ . The first has a single coupling parameter, while the second incorporates the idea of “strongly” and “weakly” coupled spins in terms of two coupling parameters. In both cases, the parameters are determined from the distribution  $P_0(J)$ . We compare the results of these two models with that obtained from the distribution  $P_0(J)$  in section III.

### 1. Single component model

In a single component model of Mn spins, where each spin is coupled in the same way to the carrier spins, the form for  $P(J)$  is just a delta function:

$$P(J) = \delta(J - J_1), \quad (18)$$

where  $J_1$  is the exchange coupling. In that case, the formulae for thermodynamic quantities derived for a distribution in the previous section lead to

$$\langle S^z \rangle = -S B_S(\beta \alpha_1), \quad (19)$$

$$\langle s^z \rangle = -j B_j(\beta \alpha^*), \quad (20)$$

with  $\alpha^* = (1/p) J \langle S^z \rangle$  and  $\alpha_1 = J_1 \langle s^z \rangle$ . The susceptibility per unit volume is

$$\chi = \chi^* + \chi_1, \quad (21)$$

and

$$\chi^* = \frac{(g^* \mu_B)^2 n_h \beta G^* \left(1 - \frac{g}{g^*} \frac{\beta}{p} J_1 G_1\right)}{1 - \frac{1}{p} \beta^2 G^* J_1^2 G_1}, \quad (22)$$

$$\chi_1 = (g \mu_B) n_{\text{Mn}} \beta G_1 \left(g \mu_B - \frac{1}{n_h} \frac{J_1}{g^* \mu_B} \chi^*\right), \quad (23)$$

where the  $G$  functions have the same meaning as previously. Finally we calculate the specific heat again with the derivative of energy with respect to temperature, but in this case the energy per Mn spin is

$$\frac{U}{N_{\text{Mn}}} = J_1 \langle S^z \rangle \langle s^z \rangle. \quad (24)$$

### 2. Two component model

As we show in the next section, the calculated distribution of exchange couplings are quite broad, and cover many orders of magnitude for parameter values of interest. This motivates us to study a model that is the next simplest after the single coupling model, namely the two component model, with an exchange distribution:

$$P(J) = \frac{n_1}{n_{\text{Mn}}} \delta(J - J_1) + \frac{n_2}{n_{\text{Mn}}} \delta(J - J_2). \quad (25)$$

The physical motivation of the above distribution is to divide the Mn spins into two types, one which is strongly coupled to the carrier spins ( $J_1$ ), with an effective concentration  $n_1$ , and the other which is weakly coupled to the carrier spins ( $J_2$ ) with a concentration  $n_2$ . Since the only energy scale characterizing the thermodynamics is the temperature  $T$ , we would expect it to play an important role in determining both the coupling constants  $J_1$  and  $J_2$ , and the concentrations of strongly and weakly coupled spins. Consequently, we expect that the best fit

to the curves for a distribution of exchanges will be obtained when  $J_i$  and  $n_i$  are temperature dependent. This temperature dependence of parameters should be viewed in the same spirit as in a variational fit to free energies of actual (T-independent) Hamiltonians by model Hamiltonians.<sup>22</sup>

We obtain a self consistent mean field solution to this model of

$$\langle S_a^z \rangle = -SB_S(\beta\alpha_a), \quad (26)$$

$$\langle s^z \rangle = -jB_j(\beta\alpha^*), \quad (27)$$

where

$$\alpha_a = J_a \langle s^z \rangle, \quad (28)$$

with  $a = 1$  or  $2$ , and

$$\alpha^* = \frac{n_1}{n_h} J_1 \langle S_{i_1}^z \rangle + \frac{n_2}{n_h} J_2 \langle S_{i_2}^z \rangle. \quad (29)$$

Using the notation introduced above, the susceptibility per unit volume is

$$\chi = \chi^* + \chi_1 + \chi_2, \quad (30)$$

where  $\chi^*$  is the contribution to the susceptibility due to the holes and  $\chi_{1,2}$  are the contributions from the two species respectively – the expressions for the susceptibilities are

$$\chi^* = \frac{(g^* \mu_B)^2 n_h \beta G^* \left( 1 - \frac{q}{g^*} \frac{n_1}{n_h} \beta J_1 G_1 - \frac{q}{g^*} \frac{n_2}{n_h} \beta J_2 G_2 \right)}{1 - \frac{1}{p} \beta^2 G^* \left( \frac{n_1}{n_{\text{Mn}}} J_1^2 G_1 + \frac{n_2}{n_{\text{Mn}}} J_2^2 G_2 \right)}, \quad (31)$$

$$\chi_a = g \mu_B n_a \beta G_a \left( g \mu_B - \frac{1}{n_h} \frac{J_a}{g^* \mu_B} \chi^* \right), \quad (32)$$

where the  $G$  functions are as defined in Equations (14) and (15). The energy per Mn spin (from which we determine the specific heat) is

$$\frac{U}{N_{\text{Mn}}} = \frac{n_1}{n_{\text{Mn}}} J_1 \langle s^z \rangle \langle S_1^z \rangle + \frac{n_2}{n_{\text{Mn}}} J_2 \langle s^z \rangle \langle S_2^z \rangle. \quad (33)$$

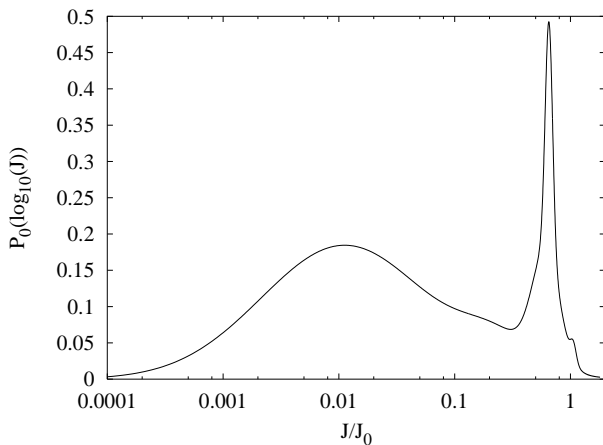


FIG. 1. The distribution  $P_0(\log_{10} J)$  calculated for  $p = 0.1$  and  $x = 0.01$  in the numerical mean field model of Ref. 13 at  $T = 0$ .

### III. NUMERICAL TESTS OF THE ONE AND TWO COMPONENT MODELS

We now compare results obtained using our simple approximations with the full numerical mean field calculations. We concentrate on two cases, where the Mn concentration  $n_{\text{Mn}}$  leads to a fractional occupancy of the Ga sublattice by Mn ions of  $x = 0.01$  and  $0.02$ . For both cases, we consider a ratio of hole concentration  $n_h$  equal to 10% of the Mn concentration, i.e.  $n_h/n_{\text{Mn}} = p = 0.1$ . The distribution  $P_0(J)$  calculated numerically<sup>13</sup> for the  $x = 0.01$  case at  $T = 0$ , using a Bohr radius for the hole equal to  $7.8 \text{ \AA}$ ,<sup>12</sup> is shown in Fig. 1. As can be seen, it spans almost three orders of magnitude, and for this density, consists of two peaks. The higher peak is due to sites where the exchange interaction is dominated by a single hole that has a high probability of being on the Mn site in question, whilst the lower peak is found to be due to sites that have practically no amplitude for a hole, but whose exchange field is coming from holes on nearby sites. As  $x$  and  $p$  are changed, the relative weights in the two peaks changes, as does the total width of the distribution. However, the inferences made for this concentration remain valid for higher values of  $x$  (we have checked explicitly the cases  $x = 0.02$  and  $x = 0.03$ ).

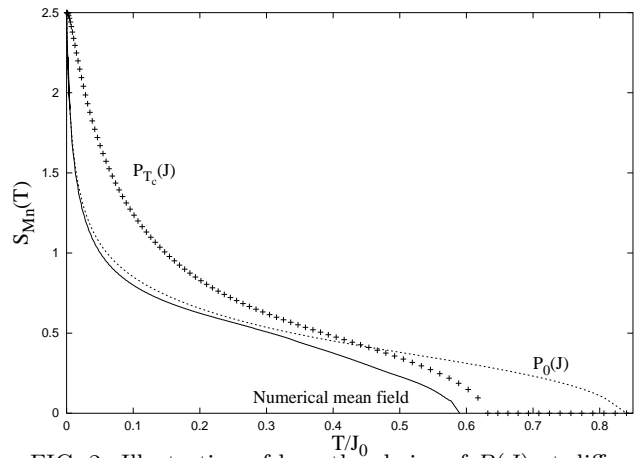


FIG. 2. Illustration of how the choice of  $P(J)$  at different temperatures for  $x = 0.01$  influences the fit to the numerical mean field magnetization curve.

Figure 2 plots the average Mn spin,  $S_{\text{Mn}}(T)$ , calculated using the self-consistent solution of section II A with the distribution  $P_0(J)$  (Fig. 1) (dashed line) and the full numerical mean field result (solid line) against temperature. As can be seen clearly, the curve using the  $T = 0$  distribution works very well (errors less than 1%) until about 60 % of  $T_c$  for the numerical mean field model. To fit the numerical results properly for higher  $T$ , one must allow for the distribution of local fields to deviate from the  $T = 0$  distribution as the polarization of the holes begins to fluctuate strongly as the transition is approached. In figure 2, we indicate with crosses the  $S_{\text{Mn}}(T)$  curve

obtained using the distribution  $P_{T_c}(J)$  (determined for  $T = T_c$ ). Clearly, an interpolation of distributions at the two extremes ( $T = 0$  and  $T = T_c$ ) will be adequate to reproduce the full numerical curve.<sup>23</sup>

Our goal is, however, to simplify the description of the distribution of exchange fields in terms of a few couplings. To this end, we consider the case with the fixed  $T$ -independent  $P(J)$  shown in Fig. 1, and attempt to fit the thermodynamic properties for that case using a one- or two- component model of Mn spins. To fit the full numerical results for temperatures up to  $T_c$  (for the numerical mean field model), we would use a similar scheme with the appropriate  $P(J)$  which best fits those numerical results. In Figures 3 to 8,  $T_c = 0.84 J_0$  refers to that determined from  $P_0(J)$  as shown in Figure 2.

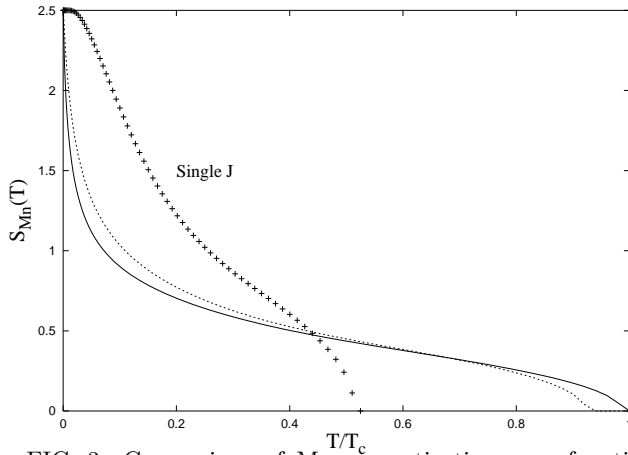


FIG. 3. Comparison of Mn magnetization as a function of temperature for the numerically derived distribution  $P(J)$  (solid line), the single coupling  $J = \bar{J}$  (labelled, crosses) model and the two component model with linear averaging (dashed line) where  $\gamma = 0.6$  and  $x = 0.01$ .

For the single coupling parameter model, we replace the distribution  $P(J)$  by the mean coupling

$$J_1 = \bar{J} = \int_0^{J_{\max}} dJ J P(J), \quad (34)$$

which for  $x = 0.01$  when we use  $P_0(J)$  gives  $\bar{J} = 0.161 J_0$ .<sup>24</sup> Figure 3 shows the average Mn spin  $S_{\text{Mn}}(T)$  (dotted curves) calculated using this model for  $x = 0.01$ . The results are clearly seen to be a poor fit to the results obtained for the full distribution (solid lines), over most of the temperature range.<sup>25</sup>

In the two-component model, the parameters are determined using the following scheme. First, since the temperature is the only thermal energy scale in the problem that can be used to define “strongly” and “weakly” coupled spins, we define a cut-off coupling  $J_c = \gamma T$ . All spins that have couplings below  $J_c$  are weakly coupled, whilst those with couplings greater than  $J_c$  are strongly coupled. Thus the concentrations  $n_1$  and  $n_2$  of the two sets of spins are given by the relative fractions of spins with couplings above and below  $J_c$ , *i.e.*:

$$\frac{n_1}{n_{\text{Mn}}} = \int_{J_c}^{J_{\max}} dJ P(J), \quad (35)$$

$$\frac{n_2}{n_{\text{Mn}}} = 1 - \frac{n_1}{n_{\text{Mn}}}. \quad (36)$$

On the other hand, the couplings  $J_1$  and  $J_2$  are taken to be the averages over the two populations

$$J_1 = \int_{J_c}^{J_{\max}} dJ J P(J), \quad (37)$$

$$J_2 = \int_{J_{\min}}^{J_c} dJ J P(J). \quad (38)$$

In this scheme, the only adjustable parameter is the dimensionless parameter  $\gamma$ , which determines  $J_c$  and is chosen to give the best overall fit to  $S_{\text{Mn}}(T)$ . Using  $P_0(J)$  yields  $\gamma = 0.6$ . Since most thermodynamic functions depend exponentially on the ratio  $J/T$ , we expect this scheme to work especially well when the distributions are broad, and the demarcation between “strongly” and “weakly” coupled spins becomes sharp.<sup>19</sup> For narrow distributions, on the other hand, this scheme essentially reduces to a single coupling, which should be adequate for most purposes.

The curve of Mn spin versus temperature  $S_{\text{Mn}}(T)$ , obtained using the two-component model, is shown in Figure 3 as a dashed line. In contrast to the single coupling model the curve has the same shape as for the full distribution and provides a much better quantitative fit. *It might appear that using two couplings to approximate the distribution shown in Fig. 1 works well because of the double peaked nature of the distribution. We wish to emphasize that this is not the case; the main reason actually appears to be the large width of the distribution  $P_0(J)$ . In particular, if the upper peak in  $P_0(J)$  is removed, then the magnetization curve from the modified  $P(J)$  still needs a two-component model to provide an adequate fit and a one-coupling parameter fit works barely better than for the distribution shown in Fig. 1.*

We now turn to other thermodynamic quantities, the susceptibility and specific heat; these quantities are shown for  $x = 0.01$  and were calculated for a distribution, as well as the single and two component models, in Section II. Figure 4 plots the susceptibility for the mean field model with the distribution  $P(J)$ , the two component model with  $\gamma = 0.6$  and the single component model for  $x = 0.01$ . Because the susceptibility is a higher order derivative, the two component model is not quite as accurate as for the magnetization. Nevertheless, there is good agreement with the results for the full distribution on a semiquantitative level down to 10 % of  $T_c$  as obtained from  $P_0(J)$ , whilst the single coupling model bears little resemblance to the distribution.

Similarly, the curves for specific heat (Fig. 5) as a function of temperature show good agreement between the two-component model and the distribution (in fact, better than for the susceptibility) for temperatures greater than  $0.1 T_c$ . In contrast, there is a strong quantitative

discrepancy between the single coupling model and the distribution. The Schottky type anomaly is broadened out considerably for the distribution as well as the two-component model; similar broadening is present in the full numerical solution.<sup>12</sup>

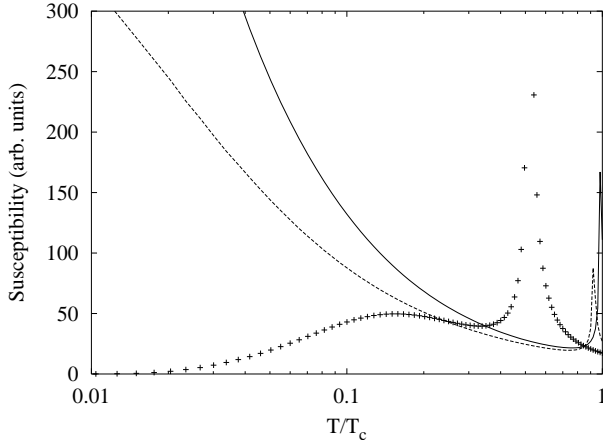


FIG. 4. Comparison of the susceptibility as a function of temperature for  $x = 0.01$  calculated for the distribution  $P(J)$  (solid line), the single coupling  $J = \bar{J}$  model (crosses) and the two component model (dashed line) with  $\gamma = 0.6$ . Note that  $T_c$  is that for  $P_0(J)$ .

Figure 4 apparently shows a divergence in the susceptibility at low temperatures – this is not a divergence, but a peak at very low temperatures, due to the considerable population of Mn spins with very small local fields.

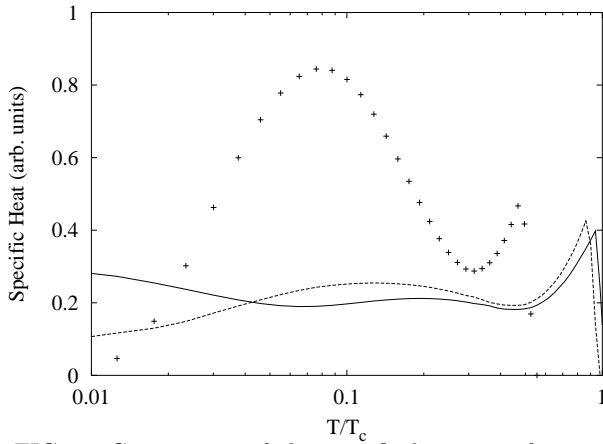


FIG. 5. Comparison of the specific heat as a function of temperature for  $x = 0.01$  calculated for the distribution  $P(J)$  (solid line), the single coupling  $J = \bar{J}$  model (crosses) and the two component model (dashed line) with  $\gamma = 0.6$ . Note that  $T_c$  is that for  $P_0(J)$ .

Finally, to understand better the behaviour of the two-coupling model, we show the temperature dependence of the couplings  $J_1$ ,  $J_2$  and  $J_c$  and also the temperature dependence of the ratio  $n_1/n_{\text{Mn}}$  in Figures 6 and 7 respectively.

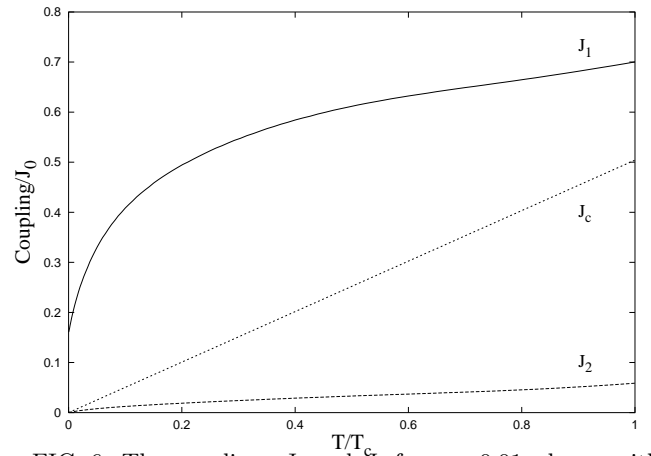


FIG. 6. The couplings  $J_1$  and  $J_2$  for  $x = 0.01$ , shown with  $J_c = 0.6T$  as functions of temperature where  $J_1$  and  $J_2$  are obtained in the linear averaging scheme. Note that  $T_c$  is that for  $P_0(J)$ .

As expected from the physically motivated criterion described earlier in this section, at low temperatures nearly all of the spins are strongly coupled; however, as the temperature rises the number of strongly coupled spins decreases sharply, as the strength of the coupling required for a spin to be strongly coupled increases with  $T$ . It is this essential aspect of a broad distribution of couplings that allows the two-component model to properly capture this behaviour.

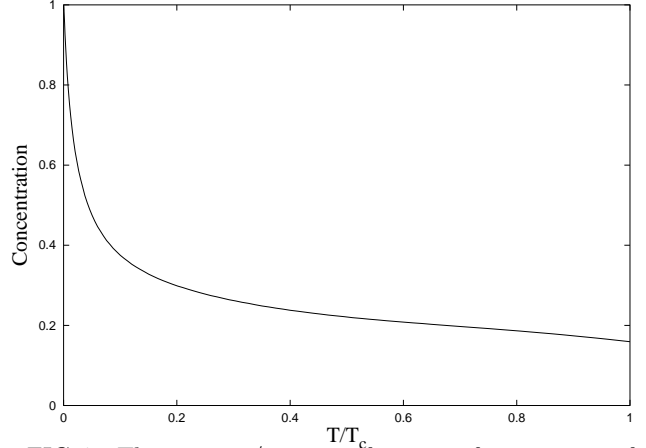


FIG. 7. The ratio  $n_1/n_{\text{Mn}}$  as a function of temperature for  $x = 0.01$  using the model in which  $J_c = 0.6T$  where  $J_1$  and  $J_2$  are obtained in the linear averaging scheme. Note that  $T_c$  is that for  $P_0(J)$ .

#### IV. DISCUSSION AND CONCLUSIONS

Whilst other authors have acknowledged that disorder plays some role in the physics of III-V DMS systems,<sup>4,11,16,17</sup> the results of mean-field<sup>12,13</sup> as well as Monte Carlo simulations<sup>14,15</sup> on models with a random distribution of dopants near the metal-insulator transi-

tion suggest that there should be strong effects on the thermodynamic properties of DMS systems, especially at low temperatures. The tendency in experimental fits, on the other hand, has been to neglect disorder effects entirely and produce fits characteristic of homogeneous systems. Thus, magnetization curves obtained from transport measurements in a sample with  $x = 0.035$ ,<sup>26</sup> are fitted with Brillouin functions to extract a single exchange coupling. It is important to ask whether the effects described here have been seen or have the potential to be seen experimentally. Significant deviations from a Brillouin curve appear to be seen in a number of experiments,<sup>5,27,28</sup> in contrast to Ref. 26. The Brillouin function-like behaviour appears to arise in transport, whilst the deviations are seen in SQUID measurements of the magnetization. One explanation for this may be that the transport measurement mainly samples Mn spins that are strongly coupled to holes, which can give a Brillouin function as described below. However, the SQUID measurement samples all Mn moments equally, and the magnetization inferred is from both weakly and strongly coupled Mn spins (as is calculated here). Interestingly, a measurement of the magnetization against magnetic field at a temperature of 2 K ( $T_c$  was 37 K) in a sample with  $x = 0.02$  showed that the magnetization was roughly only 25 % of its saturation value.<sup>29</sup> This is consistent with our picture here that due to a broad distribution of exchange couplings there are significant numbers of spins that are not polarized, even at low temperatures. In studies of insulating samples it has been observed that the saturation moment was consistent with only about 40% to 50% participation of Mn spins.<sup>30,31</sup>

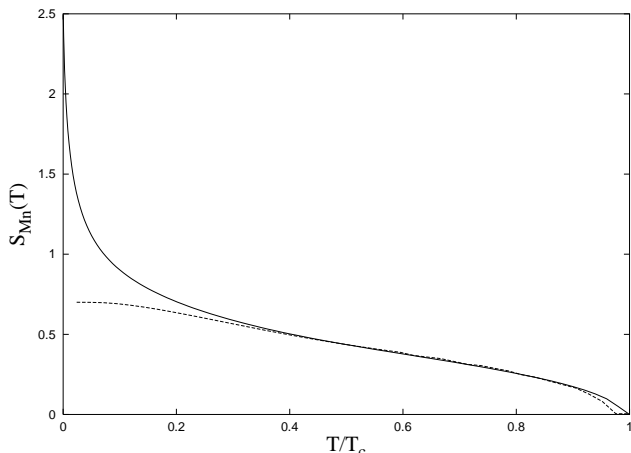


FIG. 8. Illustration of how a single Brillouin function can approximate part of the magnetization curve of a distribution ( $x = 0.01$ ). The parameters chosen for the single Brillouin function were that 28 % of the Mn spins were coupled to holes with  $J = 0.57 J_0$ , whilst the rest were uncoupled.

Figure 8 illustrates how it is possible to have the magnetization from the distribution  $P_0(J)$  fitted by a single Brillouin function over some temperature range. The pa-

rameters used to obtain the curve shown were to assume that only 28 % of the Mn spins contribute to the magnetization and that the coupling is  $J = 0.57 J_0$ . Also, in the large  $x$  insulating phase, there has been an observation of a magnetization curve that could not be fitted with a Brillouin function assuming only a single coupling.<sup>20,32</sup> In that work this was ascribed to multiple exchange mechanisms rather than disorder in the local fields as we suggest here. We believe similar effects will persist on the metallic side of the metal-insulator transition, and the assumption of a single exchange coupling used in experimental fits will be valid only deep in the metallic phase.

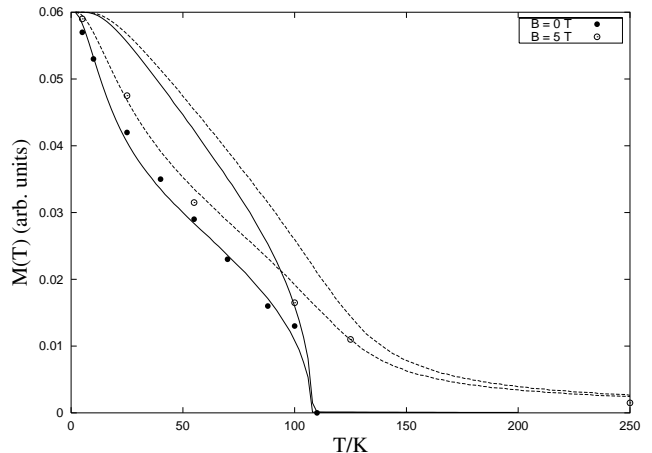


FIG. 9. Two component fit to SQUID magnetization curve at zero field and  $B = 5$  T for a sample with  $x = 0.053$  and  $p = 0.3$  from Ref. 27. The experimental data ( $\bullet$  for  $B = 0$  T, and  $\circ$  for  $B = 5$  T) is fitted very well with a two component model with  $J_1 = 47.5$  K,  $J_2 = 7.5$  K and  $n_1 = 0.41n_{Mn}$  (solid bold line for  $B = 0$  T, dashed bold line for  $B = 5$  T). The light curves are for a single coupling and  $J = 31$  K (solid  $B = 0$  T and dashed  $B = 5$  T).

To illustrate this point, we show data for the remanent magnetization and field dependent magnetization from a SQUID measurement (Ref. 27) for a sample with  $x = 0.053$  and  $p = 0.30$  that has been fit with  $j = 3/2$  at zero field and at  $B = 5$  T. (Note that the only change required to include a magnetic field in the formalism in Section II, is  $\alpha \rightarrow \alpha - g\mu_B B$ ). Since we obviously do not know  $P(J)$  in this case, and we expect it to be less broad in the metallic phase, we have taken temperature independent  $J_1$ ,  $J_2$  and  $n_1$ , and compared the fit to one with a single  $J$  that reproduces  $T_c$  correctly. Using  $J_1 = 47.5$  K,  $J_2 = 7.5$  K and  $n_1 = 0.41n_{Mn}$  we obtain the fits shown in Fig. 9 as bold solid and dashed lines, which are in close accord with the data at both magnetic field strengths, whereas a fit with a single  $J = 31$  K (light and solid dashed lines) is clearly inadequate. Whilst a single fit of this form does not necessarily imply our model, it would clearly be of use to determine if a such a two component behaviour is universally seen, by fitting experimental data for  $M(H, T)$  at several fields and temperatures.



In conclusion, we have found that we can approximate the results of the numerical mean field treatment of a kinetic-exchange model of Mn dopants in GaAs, which properly treats the positional disorder in the alloy system, by a simple exchange model with temperature-dependent effective couplings between carriers and two different species of Mn spins. Such a model emerges naturally because of the distribution of couplings that are a consequence of the positional disorder of the Mn ions. Since the ultimate inputs in the simple model are the couplings  $J_i$  and concentrations  $n_i$  of each species, by parametrizing the behavior shown in Figures 7 and 8 in terms of a single parameter (or perhaps two), experimental data can be used to yield information about the true nature of coupling distributions in actual DMS materials. We hope that with more detailed measurements, both of bulk magnetic and thermodynamic quantities, as well as those from local probes, it may be possible to parametrize the couplings accurately enough to provide a quantitative fit to the other thermodynamic properties at various concentrations in all regions of the phase diagram, in the quantitative manner possible for crystalline systems with translational symmetry.

## V. ACKNOWLEDGEMENTS

We acknowledge many useful discussions with Xin Wan. This project was supported by NSF DMR-9809483. MB acknowledges Postdoctoral Fellowship support from the Natural Sciences and Engineering Research Council of Canada. RNB thanks the Isaac Newton Institute, Cambridge University, and the Aspen Center for Physics for hospitality during the initial stages of this work.

## APPENDIX A: DERIVATION OF INTEGRAL OVER EFFECTIVE COUPLINGS

The Hamiltonian (Eq. (2)) may be rewritten as

$$\mathcal{H} = J_0 \sum_{i\alpha} |\phi_\alpha(\mathbf{R}_i)|^2 \mathbf{s}_\alpha \cdot \mathbf{S}_i, \quad (\text{A1})$$

where we have used the definition  $J_{i\alpha}(\mathbf{R}_i) = J_0 |\phi_\alpha(\mathbf{R}_i)|^2$ . We assume that the amplitude of the  $\alpha^{\text{th}}$  hole at site  $i$  may be written as the sum over Mn sites of the product of the amplitude for a hole to be at a given site times the amplitude from the local atomic orbital  $\psi(r)$  (note that  $\psi(r) \propto e^{-r/a_B}$ ). Hence

$$|\phi_\alpha(\mathbf{R}_i)|^2 = \sum_j p_\alpha(\mathbf{R}_j) |\psi(\mathbf{R}_i - \mathbf{R}_j)|^2, \quad (\text{A2})$$

where we are in effect ignoring any quantum interference terms. This allows us to rewrite the Hamiltonian as

$$\mathcal{H} = J_0 \sum_{ij\alpha} p_\alpha(\mathbf{R}_j) |\psi(\mathbf{R}_i - \mathbf{R}_j)|^2 \mathbf{s}_\alpha \cdot \mathbf{S}_i. \quad (\text{A3})$$

One of our mean field assumptions (based on the idea that each hole interacts with many Mn spins<sup>13</sup>), is that each hole behaves identically – in which case,  $\langle \mathbf{s}_\alpha \rangle = \langle \mathbf{s} \rangle$  independent of  $\alpha$ . This also means that  $p_\alpha(\mathbf{R}_j) = (1/N_h)p(\mathbf{R}_j)$ , where  $p(\mathbf{R}_j)$  is the amplitude for finding *any* hole at site  $i$ .

If we define

$$J_i = J_0 \sum_j p(\mathbf{R}_j) |\psi(\mathbf{R}_i - \mathbf{R}_j)|^2, \quad (\text{A4})$$

then the effective exchange field at site  $i$  is  $J_i$  and the Hamiltonian takes the form

$$\mathcal{H} = \sum_i J_i \mathbf{s} \cdot \mathbf{S}_i. \quad (\text{A5})$$

To convert this sum into an integral, define

$$P(J) = \frac{1}{N_{\text{Mn}}} \sum_i \delta(J - J_i). \quad (\text{A6})$$

In mean field,  $\langle \mathbf{S}_i \rangle$  depends only on  $J_i$ , hence we can relabel  $S_i = S_J$  and the Hamiltonian takes the form of Eq. (4) when we use the identity

$$\int_0^{J_{\text{max}}} dJ P(J) = 1. \quad (\text{A7})$$

- 
- <sup>1</sup> H. Ohno, Science **281**, 951 (1998).
  - <sup>2</sup> G. A. Prinz, Science **282**, 1660 (1998).
  - <sup>3</sup> F. Matsukura, H. Ohno, A. Shen, and Y. Sugawara, Phys. Rev. B **57**, R2037 (1998).
  - <sup>4</sup> T. Dietl and H. Ohno, Physica **E9**, 185 (2001); T. Dietl, H. Ohno, and F. Matsukura, Phys. Rev. B **63**, 195205 (2001).
  - <sup>5</sup> B. Beschoten, P. A. Crowell, I. Malajovich, D. D. Awschalom, F. Matsukura, A. Shen, and H. Ohno, Phys. Rev. Lett. **83**, 3073 (1999).
  - <sup>6</sup> H. Ohno, J. Magn. Magn. Mat. **200**, 110 (1999).
  - <sup>7</sup> J. Szczytko, W. Mac, A. Twardowski, F. Matsukura, and H. Ohno, Phys. Rev. B **59**, 12 935 (1999).
  - <sup>8</sup> T. Dietl, J. Cibert, P. Kossacki, D. Ferrand, S. Tatarenko, A. Wasiela, Y. Merle d'Aubigné, F. Matsukura, N. Akiba, and H. Ohno, Physica **E7**, 967 (2000).
  - <sup>9</sup> J. König, H.-H. Lin, and A. H. MacDonald, Phys. Rev. Lett. **84**, 5628 (2000); cond-mat/0010471.
  - <sup>10</sup> M.-F. Yang, S.-J. Sun, and M.-C. Chang, Phys. Rev. Lett. **86**, 5636 (2001); J. König, H.-H. Lin, and A. H. MacDonald, Phys. Rev. Lett. **86**, 5637 (2001).
  - <sup>11</sup> J. Schliemann, J. König, H.-H. Lin, and A. H. MacDonald, Appl. Phys. Lett. **78**, 1550 (2001).
  - <sup>12</sup> M. Berciu and R. N. Bhatt, Phys. Rev. Lett. **87**, 107203 (2001).
  - <sup>13</sup> M. Berciu and R. N. Bhatt, cond-mat/0111045.

- <sup>14</sup> R. N. Bhatt and X. Wan, Int. J. Mod. Phys. C **10**, 1459 (1999).
- <sup>15</sup> X. Wan and R. N. Bhatt, cond-mat/0009161.
- <sup>16</sup> M. A. Boselli, A. Ghazali, and I. C. da Cunha Lima, Phys. Rev. B **62**, 8895 (2000)
- <sup>17</sup> J. Schliemann, J. König, and A. H. Macdonald, Phys. Rev. B **64**, 165201 (2001).
- <sup>18</sup> R. N. Bhatt and P. A. Lee, Phys. Rev. Lett. **48**, 344 (1982).
- <sup>19</sup> R. N. Bhatt, Physica Scripta **T14**, 7 (1986).
- <sup>20</sup> A. Van Esch, L. Van Bockstal, J. De Boeck, G. Verbanck, A. S. van Steenberghe, P. J. Wellmann, B. Grietens, R. Bogaerts, F. Herlach, and G. Borghs, Phys. Rev. B **56**, 13103 (1997).
- <sup>21</sup> J. Schneider, U. Kaufmann, W. Wilkening, M. Baeumler, and F. Kohl, Phys. Rev. Lett. **59**, 240 (1987).
- <sup>22</sup> R. P Feynman, *Statistical Mechanics*, (Benjamin, 1972) pp 47, 67-71.
- <sup>23</sup> Interestingly, because spin 3/2 holes lead to a lower  $T_c$  than spin 1/2 holes, the magnetization curves for spin 3/2 holes using the distribution  $P_0(J)$  overlap almost perfectly with the numerical mean field theory (with spin-1/2 holes) for all  $T$ .
- <sup>24</sup> It may appear from the equation for  $T_c$ , (Eq. (10)) that we should fit the r.m.s exchange coupling. This would lead to minor modifications to  $T_c$ ; however the significant difference in shape of  $S_{Mn}(T)$  curves cannot be rectified by adjusting  $T_c$ .
- <sup>25</sup> The same quality of fit is seen for  $x = 0.02$  or  $x = 0.03$ .
- <sup>26</sup> H. Ohno, N. Akiba, F. Matsukura, A. Shen, K Ohntani, and Y. Ohno, Appl. Phys. Lett. **73**, 363 (1998).
- <sup>27</sup> H. Ohno and F. Matsukura, Solid State Commun. **117**, 179 (2001) – see their Fig. 2(b).
- <sup>28</sup> J. G. E. Harris, D. D. Awschalom, F. Matsukura, H. Ohno, K. D. Maranowski, and A. C. Gossard, Appl. Phys. Lett. **75**, 1140 (1999).
- <sup>29</sup> H. Ohldag, V. Solinus, F. U. Hillebrecht, J. B. Goedkoop, M. Finazzi, F. Matsukura, and H. Ohno, Appl. Phys. Lett. **76**, 2928 (2000).
- <sup>30</sup> A. Oiwa, S. Katsumoto, A. Endo, M. Hirasawa, Y. Iye, H. Ohno, F. Matsukura, A. Shen, and Y. Sugawara, Solid State Commun. **103**, 209 (1997).
- <sup>31</sup> H. Nojiri, M. Motokawa, S. Takeyama, F. Matsukura, and H. Ohno, Physica B **256-258**, 569 (1998).
- <sup>32</sup> L. Van Bockstal, A. Van Esch, R. Bogaerts, F. Herlach, A. van Steenberghe, J. De Boeck, and G. Borghs, Physica **B246**, 258 (1998).